Study of Mechanical Properties of Weldments by Impression Tests

Impression test results are found to be compatible with conventional hardness and tensile test results

BY H. Y. YU, M. A. IMAM, AND B. B. RATH

ABSTRACT. The mechanical properties of high energy laser beam welds in A36 steel were studied using impression tests in which a flat-end circular cylindrical indenter of 1 mm (0.04 in.) diameter is penetrated into the specimen at a constant speed. The yield strength, ultimate tensile strength, strain-rate sensitivity, strain-hardening coefficients and elongations for various zones of the weldments obtained by the present study are reported. The results are compared with the conventional tensile and hardness tests.

Introduction

Measuring the strength and ductility properties of weldments can be a very difficult and often impossible task. Standard methods using round or flat tensile specimens cut transverse to weldments often fail in base metal, yielding only the information that fusion zone (FZ) and heat-affected zone (HAZ) strengths exceed that of the base metal (BM). Even when failures occur in the FZ, data describing ductility are inconclusive because of unsymmetrical flow due to local differences in metal properties. All-weld-metal samples taken from very wide gap weldments are not conclusive because of directionality effects, which can be significant. These problems hamper welding development programs, because conclusive data to compare different weld metal compositions, welded joint geometries and combinations of these are not easily obtainable.

One method of obtaining local mechanical properties of weldments is by impression measurements. The operating principle of impression methodology is that the flow properties of a small volume of material can be characterized by its resistance to indentation. These methods have existed for many years, and considerable work has been done to develop them. Results have been conflicting in nature, because the methods used for loading and data analyses have been inconsistent and the response of materials to local loading and indenter geometry have been poorly understood (Refs. 1-7). Recent work (Refs. 8-10), however, has shown that by using consistent loading and data reduction methods, a correlation between material behavior in standard tests and the local response to impression can be developed. Using such correlations, it is possible to delineate the individual properties of FZ, HAZ and BM in a weldment.

H. Y. YU is with the Chung Cheng Institute of Technology, Taiwan, and M. A. IMAM and B. B. RATH are with the Naval Research Laboratory, Washington, DC.

Experimental Procedure

The material selected for this investigation was a laser beam weld in the most widely used weldable structural steel in this country, conforming to the ASTM specification A-36 (0.20 wt-% C, 1.00 wt-% Mn). A 12 mm (0.47 in.) thick A-36 steel plate was welded with a laser beam operated at 13 kW power. The FZ of the weldments was about 3.5 mm (0.14 in.) wide. Rectangular block specimens with 40 × 25 × 12 mm (1.57 × 0.98 × 0.47 in.) dimensions were cut transverse from the as-welded weldment.

The HAZ of the weldment had a refined, small grain size, ferrite/pearlite structure, whereas the FZ had a bainite structure. The average grain size in each zone was less than 50 μm (0.002 in.). Some of the specimens were annealed at 635°C (1175°F) for one hour (h) to remove the residual stresses. Both the as-welded and the annealed specimens were mechanically polished and etched with 1% nital solution to reveal the different zones. The details of A-36 laser beam welding, microstructure, and results of mechanical tests were given by Metzbower and Moon (Refs. 11,12).

The testing arrangement for impression test is shown schematically in Fig. 1. A flat end cylindrical punch of 1 mm (0.04 in.) diameter, machined from tungsten carbide rod, was used for the impression test. The test was done at room temperature in a closed-loop hydraulic testing machine. The load signal from the hydraulic testing machine and the corresponding displacement of the punch or the penetration signal from the output of a linear variable differential transformer (LVDT), attached between load cell and

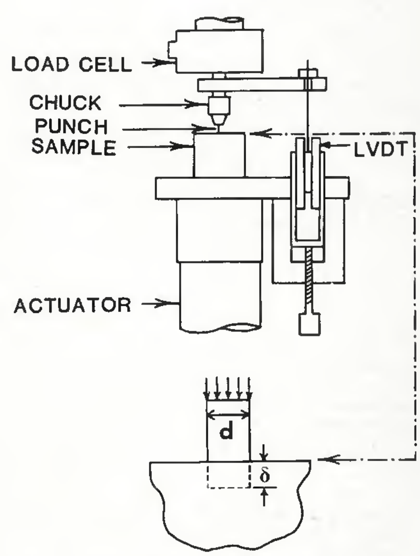

Fig. 1—Schematic of test arrangement for impression test

the sample, were recorded simultaneously during the test by an x-y recorder.

To study the flow behavior, an arbitrary penetration speed of 8.5×10^{-4}mm/s (0.002 ipm) was used. This was equivalent to true strain rate of $1.275 \times 10^{-3}s^{-1}$. For strain rate sensitivity measurements, penetration speeds of 8.5×10^{-4}mm/s (0.002 ipm) and 8.5×10^{-3}mm/s (0.02 ipm) were used. The FZ impression test was carried out with an indentation approximately 3.5 mm (0.14 in.) apart, whereas a 10 mm (0.39 in.) distance from the FZ center was chosen to study the BM.

Since there was no sharp boundary between HAZ and FZ or HAZ and BM, the impression tests of HAZ were carried out arbitrarily at the edge of the FZ. Moreover, the HAZ was not homogeneous, and as such the results obtained were some average properties of HAZ.

Results and Discussion

By comparing the flow curves obtained by compression and impression tests, one can establish a correlation between the true stress, σ, and the true strain, ϵ, in compression and stress, P, (load divided by the uniform cross-section area of the indenter) and normalized penetration, δ/d, (δ is the penetration depth and d is the diameter of the indenter) in impression. These correlations for mild steel were found to be (Ref. 9):

$$\sigma = P/2.9 \quad (1)$$

$$\epsilon = 1.5\frac{\delta}{d} \quad (2)$$

The data for stress, P, and normalized penetration, δ/d, obtained by averaging results of five impression tests, were transformed into true stress, σ, and true strain, ϵ, using equations (1) and (2). Figure 2 is a plot of true stress, σ, versus true strain, ϵ, on a linear scale for both as-welded and stress-relieved conditions.

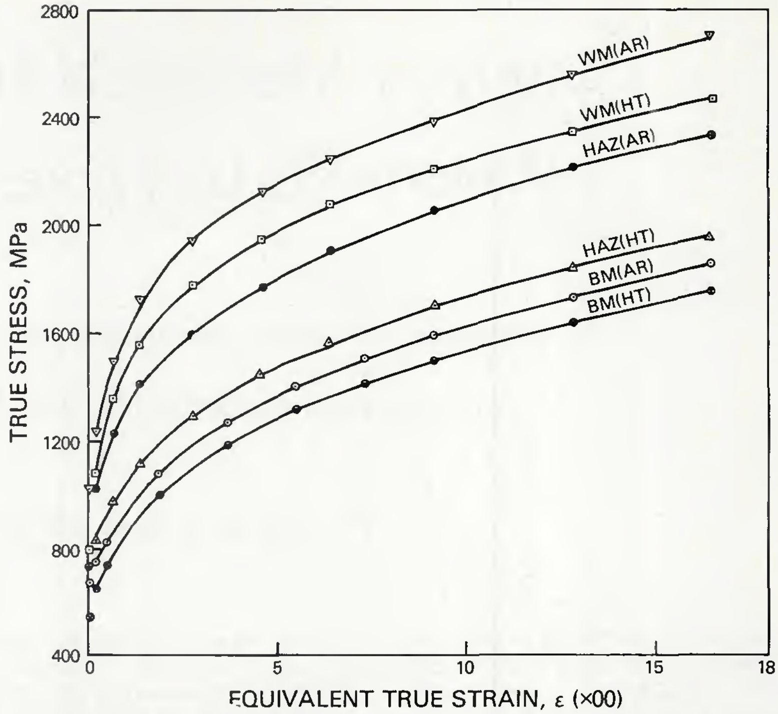

Fig. 2 — True stress vs equivalent true plastic strain curves for BM, HAZ and FZ in A36 laser beam weldments — as-welded (AR) and with stress relief (HT)

The reproducibility of the impression tests was very good in both the BM and FZ, whereas the results with the HAZ showed variations between the results of FZ and BM. The scatter in the results with the HAZ was expected because of the inhomogeneity of the zone. Since there was scatter in the results of HAZ from one location to another, the impression test results of only one specific location in HAZ are plotted in Fig. 2. The yield strength of BM, HAZ and FZ based on 0.2% offset was determined from the curves in Fig. 2, and the results — together with other properties — are shown in Table 1.

The ultimate strength was determined by using Considere's construction (Ref. 13). The Considere's construction for the base metal only was constructed from the flow curve of Fig. 2 and is shown in

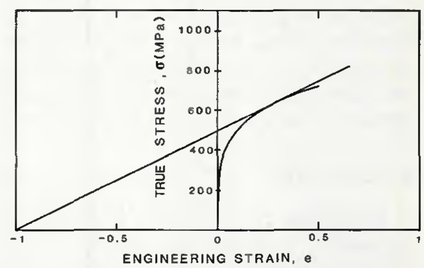

Fig. 3 — Considere's construction for determining the ultimate strength (e.g., base metal) from the flow curve of Fig. 2

Fig. 3. The x-axis in Considere's construction was engineering strain e, which was obtained by the relation:

$$e = \exp(\epsilon) - 1 \quad (3)$$

Table 1—Mechanical Properties of Laser Welded A-36 Steel

		0.2% Yield strength		Ultimate strength		Strain-rate Sensitivity,	Strain-hardening coefficient,	Theoretical elongation
		MPa	(ksi)	MPa	(ksi)	m	n	(μ = 0.005), %
Base metal	As-welded	262	(38)	496	(72)	0.0101	0.244	30
	Stress-relieved	228	(33)	472	(68)	0.0106	0.253	32
Fusion zone	As-welded	428	(62)	725	(105)	0.0054	0.177	19
	Stress-relieved	385	(56)	665	(96)	0.0060	0.186	20
HAZ	As-welded	367	(52)	628	(91)	0.0063	0.204	23
	Stress-relieved	292	(42)	528	(77)	0.0094	0.227	28
Transverse tension specimen[a]	As-welded	276	(40)	448	(65)	—	—	24

[a]Metzbower results (Ref. 11).

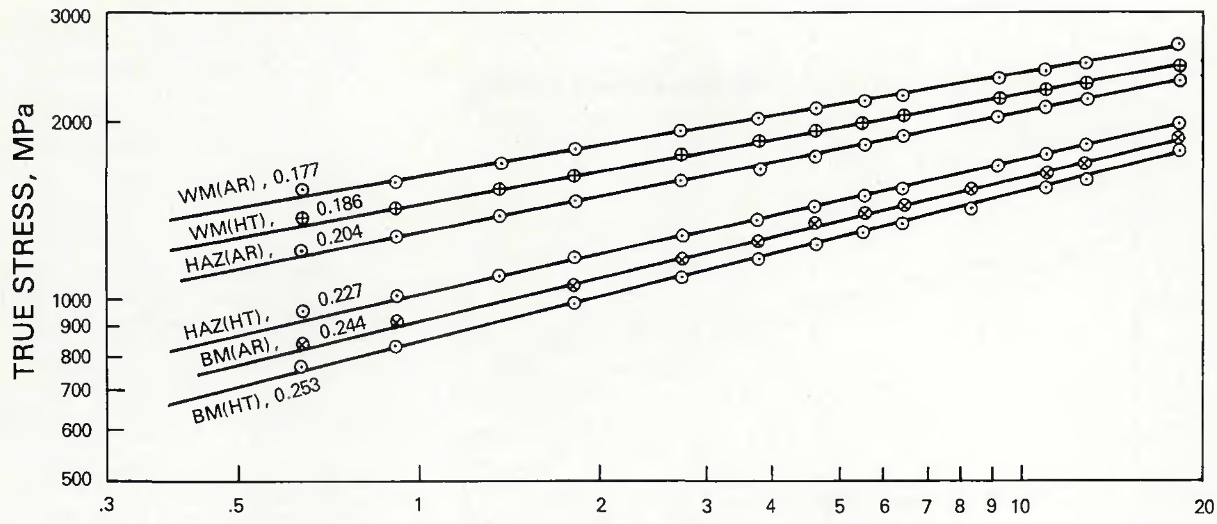

Fig. 4 — Log-log plot of the true stress vs. equivalent true plastic strain of the curves shown in Fig. 2

The ultimate strengths obtained for BM, HAZ and FZ are shown in Table 1.

The strain rate sensitivity, m, measurements for BM, HAZ and FZ were evaluated by using the following relationship:

$$m = \frac{\ln(\sigma_2/\sigma_1)}{\ln(\dot{\epsilon}_2/\dot{\epsilon}_1)}\Bigg|_{\epsilon, T = R \cdot T} \qquad (4)$$

where $\dot{\epsilon}_1 = 1.275 \times 10^{-3}$ s^{-1}, $\dot{\epsilon}_2 = 1.275 \times 10^{-2}$ s^{-1}, and σ_1 and σ_2 referred to the stresses corresponding to strains of ϵ_1 and ϵ_2, respectively. The results of strain rate sensitivity measurements are given in Table 1.

Figure 4 is a log-log plot of the true stress vs. true strain curves shown in Fig. 2 with strains larger than 1%. The results in Fig. 4 show straight lines, meaning the flow character of the different zones of the weldment in the as-welded and stress-relief conditions followed the following power law:

$$\sigma = K\epsilon^n \qquad (5)$$

where K is the strength coefficient and n is the strain hardening coefficient.

The slopes of the straight lines shown in Fig. 4 were determined and gave the value of strain hardening coefficient in equation (5). The results of strain hardening coefficient obtained from Fig. 4 for BM, HAZ and FZ of both as-welded and stress-relief conditions were shown in Table 1.

The results for yield strength and ultimate strength shown in Table 1 indicated a decreasing value from FZ to BM. These results were compatible to Vicker hardness results of Metzbower (Ref. 11) taken across the laser beam weldments as shown in Fig. 5. The ratio of yield strength for the FZ to that of the BM was 1.64, which was exactly the same as that obtained from hardness measurements of FZ and BM.

The transverse-tension test results of the as-welded specimen were reported by Metzbower (Ref. 11) and are shown in Table 1. The yield strength and the ultimate strength of BM were found to be 276 and 448 MPa (40 and 65 ksi), respectively. From impression tests, the yield strength and the ultimate strength were found to be 262 and 496 MPa (38 and 72 ksi), respectively. Thus, the results of the two tests were compatible.

Stress relieving lowered the yield strength of the BM by about 13% and that of the FZ by about 10%, whereas the ultimate strength of BM was lowered by 6% and that of the FZ by about 9%. Hence, the effect of annealing (stress-relief) was more on yield strength than in ultimate strength. The annealing effect on ultimate strength of the FZ was more than on the BM, whereas the yield strength of BM was more affected than was the FZ.

The test of weldment ductility was a major concern. Among the factors that influence necking or strain localization in metals under tension are the work hardening properties of the material and its strain rate sensitivity. Woodford (Ref. 14) had shown a correlation between strain rate sensitivity and total elongation at rupture for a number of materials and showed that some relation existed between the elongation and strain-rate sensitivity. Hutchinson and Neale (Ref. 15), using a nonlinear analysis for long-wavelength nonuniformities, showed that:

$$\int_0^{\infty} e^{-st}\, t^P dt = \frac{1}{(1-\mu)^s} \int_0^{\epsilon_o^c} e^{-st}\, t^P dt \qquad (6)$$

where s = 1/m, m is strain rate sensitivity; P = n/m, n is strain hardening coefficient; $\mu = (A_o - A)/A_o$ is the initial fractional nonuniformity in cross-section area; ϵ_o^c = called critical strain and is the uniform strain in the uniform region when the strain in the local or nonuniform section becomes infinite; A_o = the initial cross-section area of the uniform region; A = the initial cross-section area of the smallest cross-section in the nonuniform region.

By using equation (6) and correlating the critical strain, ϵ_o^c, to the engineering strain, e, determined by:

$$e = \exp(\epsilon_o^c) - 1 \qquad (7)$$

Hutchinson and Neale showed that the effect of strain rate sensitivity on elongation at rupture (from Woodford's (Ref. 14) compilation of experimental data for a variety of materials) lies in the range of numerical results predicted by their analysis. Therefore, equations (6) and (7) can be used as a reasonable estimation of the elongation of strain-rate sensitive materials under tension test. Equation (6)

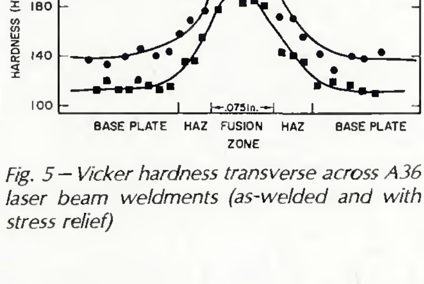

Fig. 5 — Vicker hardness transverse across A36 laser beam weldments (as-welded and with stress relief)

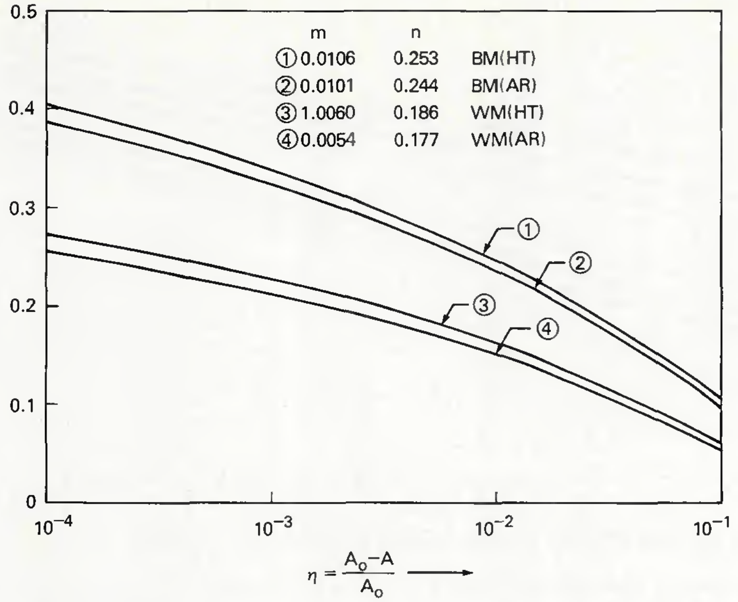

Fig. 6 — Estimated elongation in terms of non-uniformity, μ, with different n and m values (given in Table 1)

has been rewritten (Ref. 10) in the form:

$$P^m(x^2/\nu) = 1 - \mu \quad (8)$$

where $P(x^2/\nu)$ is the chi-squared probability distribution function; $x^2 = 2(\epsilon_0^c/m)$ is the upper integration limit for which the probability is computed; $\nu = 2(n/m + 1)$ is the degree of fraction of the chi-square distribution.

A subroutine for the calculation of $P(x^2/\nu)$ can be found in the IMSL (International Mathematical and Statistical Libraries) subroutine package. The estimated elongation in terms of nonuniformity, μ, with different n and m values (given in Table 1) is shown in Fig. 6. The estimated elongations with μ equal to 0.005 (reasonable for nonhomogeneities introduced during machining of a tensile specimen) are given in Table 1. The elongation of the tension test is 24%, which is less than the estimated elongation of base metal (30%) and larger than the estimated value (19%) of the fusion zone.

The transverse-tension specimens of weldment can be treated as laminates of different composition with tension load applied perpendicular to the laminate plane. Hence, an isostress approach can be used and the resulting strain should be between the strain of laminate materials (BM, HAZ and FZ).

Conclusions

1. Results from an impression test method to study mechanical properties such as yield strength, ultimate strength, strain hardening coefficient, and strain rate sensitivity of weldments are found to be compatible with conventional hardness and tension test results.

2. This method can be used to evaluate the mechanical properties of the fusion zone, heat-affected zone, and base metal of weldments.

Acknowledgment

The A36 laser weldment supplied by Dr. E. A. Metzbower and Dr. D. W. Moon is acknowledged.

References

1. Sachs, G. 1931. *Mitt. d. Deut. Mat. Pruf.* 16: 96.
2. O'Neill, H., and Greenwood, H. 1932. *J. Inst. Metals* 48: 47.
3. Hencky, H. 1923. *Angew Math. Mech.* 3: 241.
4. Ishlinsky, A. J. 1944. *J. Appl. Math. Mech. (U.S.S.R.)* 8: 233.
5. Shiled, R. T. 1956. *Proc. Royal Soc. London* 233: 267.
6. Eason, G., and Shield, R. T. 1960. *Angew Math. Phys.* 11: 33.
7. O'Neill. 1967. Hardness measurement of metals and alloys, 2nd edition: 10. London: Chapman and Hall.
8. Chu, S. N. G., and Li, J. C. M. 1980. *Mat. Sci. Eng.* 45: 167.
9. Yu, H. Y., Imam, M. A., and Rath, B. B. 1984. Study of the deformation behavior of homogeneous materials by impression tests, *J. Mat. Sci.* (in press).
10. Yu, H. Y., Imam, M. A. and Rath, B. B. 1984. Strain rate sensitivity measurement by impression method, to be published.
11. Metzbower, E. A. 1983. Laser welding of mild steel at NIROP. Minneapolis, NRL report 8626.
12. Metzbower, E. A., and Moon, D. W. 1981. Laser in metallurgy: 255. Chicago: AIME.
13. Considere, A. 1885. *Ann. Ponts Chaussees* 9: 574.
14. Woodford, D. A. 1969. *Trans. ASM* 62: 291.
15. Hutchinson, J. W., and Neale, K. W. 1977. *Acta Met.* 25: 839.